

(Interscience Publishers, Inc., New York, 1963).

⁴M. Neugebauer and C. W. Snyder, *Science* **138**, 1095 (1962).

⁵C. W. Snyder and M. Neugebauer, Fourth International Space Science Symposium (Cospar), Warsaw, 1963 (unpublished).

⁶The post-shock gas velocity used is that when the magnetic field appears to have stabilized to its new value after the initial pulse has passed.

⁷W. B. Thompson, *An Introduction to Plasma Physics* (Pergamon Press, New York, 1962), p. 92.

⁸M. Neugebauer, private communication.

TIME-SPACE RESOLVED EXPERIMENTAL DIAGNOSTICS OF THETA-PINCH PLASMA BY FARADAY ROTATION OF INFRARED He-Ne MASER RADIATION*

Arwin A. Dougal, John P. Craig, and Robert F. Gribble
The University of Texas, Austin, Texas

(Received 25 June 1964)

We report an experimental method for time-space resolved measurements on a dense, extreme-temperature, plasma in a theta pinch by observation of Faraday rotation of 3.39μ infrared He-Ne maser radiation. Since the rotation is proportional to B , this method affords a powerful technique for measuring B in pure, fully ionized, hydrogenic plasmas as occur in controlled fusion research when electron density n is determined independently. A unique feature of the method is the successful utilization of a low-power (2-mW) CW gas-phase maser to extreme temperature plasma diagnostics. Seven degrees of rotation along the central axis are observed at the $3.5\text{-}\mu\text{sec}$, 50 000-gauss, peak field compressing fully ionized deuterium at an initial electron density of $6 \times 10^{15}/\text{cm}^3$, and immersed in a 4500-gauss forward bias field. The results confirm earlier considerations^{1,2} and expectations that the coherence, monochromaticity, and low beam divergence properties of infrared and optical masers could be effectively utilized for magnetoplasma diagnostics.

The experimental arrangement, found to be highly versatile and accurate, is shown in Fig. 1. 2 mW of 3.39μ linearly polarized radiation is delivered in the output beam of the He-Ne gas-

phase maser which utilizes a metal-coated spherical mirror and a silicon flat for the infrared resonator. A first pair of flat and spherical mirrors focuses the beam to less than 1-mm diameter at the center of the theta-pinch plasma tube. A second pair of flat and spherical mirrors directs the emerging beam in turn through a 3.39-IR narrow band pass filter, and iris, and focuses it onto a polarization analyzer. The second spherical mirror provides compensation for beam refraction that is observed to occur due to radial electron-density variations.

A time-resolving infrared polarization analyzer for the 2- to 4-micron range was developed for this investigation.³ The instrument employs two Brewster-angle, air-germanium interfaces positioned such that the parallel and perpendicular components of the polarized radiation are directed onto two separate uncooled InAs photovoltaic detectors. Angular resolution of approximately 0.5° for polarization oscillations as high as 1 Mc/sec is obtained for 0.5 mW into the analyzer. In this application the analyzer is positioned at 45° relative to the nonrotated polarization to provide equal intensity onto the detectors. The preamplified detector outputs are both added and subtracted, with the sum $S(t)$ and difference $D(t)$ simultaneously displayed on the dual-beam oscilloscope. As Faraday rotation is effected by the plasma, the angular rotation θ_r is given by

$$\theta_r(t) = \frac{1}{2} \arcsin[D(t)/S(t)] \quad (1)$$

Deuterium is initially fully ionized within the 20-cm length, 5-cm ID, coil by super high-power 50 MW preheating at 1.5 Mc/sec.⁴ A forward or reverse B_0 bias field to 10 kG is provided. magnetic compression is achieved by $3.5\text{-}\mu\text{sec}$ rise to a peak as high as 75 kG.⁵

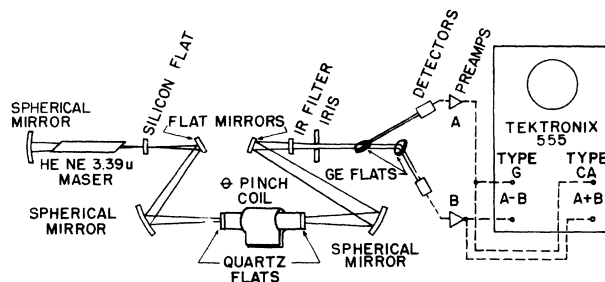


FIG. 1. Faraday-rotation arrangement for IR maser diagnostics of theta-pinch plasma.

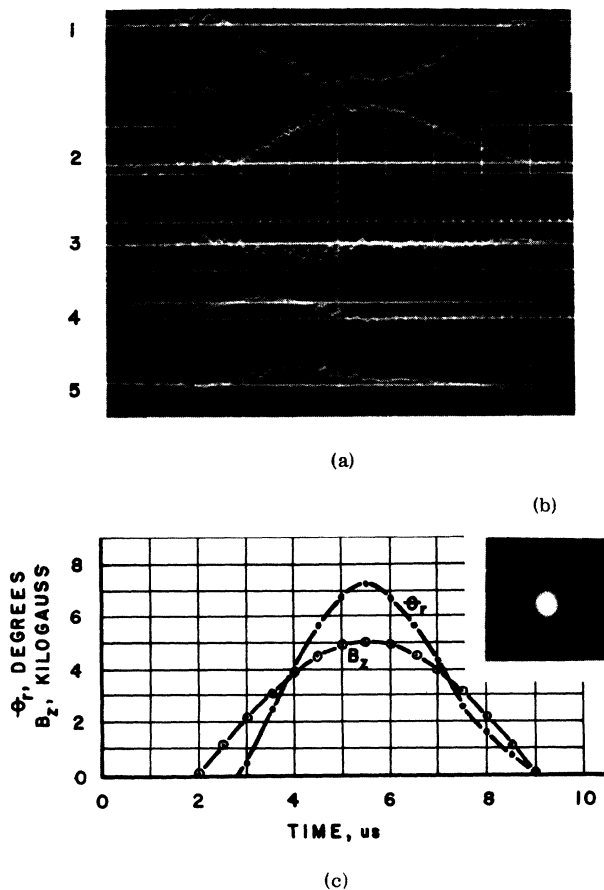


FIG. 2. Faraday-rotation results for beam positioned on central axis. Traces 2 and 4 of (a), $1 \mu\text{sec}/\text{div}$, are difference and sum, respectively. Trace 1 is a repeat difference for the analyzer rotated 90° . Traces 3 and 5 are difference and sum in the absence of the maser beam. Amplitudes are $250 \mu\text{V}/\text{div}$ and $1.25 \text{ mV}/\text{div}$ for the difference and sum traces, respectively. (b) is a Kerr cell photograph of the compressed plasma column at the instant of peak compressing field. θ_r of (c) is calculated from traces 2 and 5 and plotted with the compression field of 50-kG peak.

A Kerr cell photograph of the luminous compressed plasma column taken at the peak of the compression field is shown in Fig. 2(b). Deuterium at 0.1 Torr, fully ionized, in 4.5-kG forward bias field, is compressed with a peak field of 50 kG. Compression to $\frac{1}{4}$ of the tube radius is observed. Faraday rotation for the maser beam positioned on the center line of this compressed plasma column is observed from traces 2 and 4 in Fig. 2(a), which are difference and sum signals, respectively. Traces 3 and 5 are corresponding difference and sum signals, respectively, in the absence of the maser beam. θ_r determined from these traces and Eq. (1) is

shown in Fig. 2(c) with the compression field. Note that maximum rotation of 7° occurs at the 50 000-kG compression-field peak.

To verify that the observation is Faraday rotation, the analyzer was rotated 90° and the difference signal, trace 1, was obtained for the same experimental conditions. Trace 1 is the negative of trace 2. Amplitude scales are $250 \mu\text{V}/\text{div}$ and $1.25 \text{ mV}/\text{div}$ for the difference and sum traces, respectively. The initial sum amplitude was 1.7 mV.

θ_r is related to the plasma properties through^{1,2}

$$\theta_r = (3.02)10^{-24}Bln \text{ radian}, \quad (2)$$

where B is the field in gauss, l is the plasma column length of 20 cm, and n is the electron density in cm^{-3} . In Eq. (2) θ_r is simplified from an integral over l of the product $B(l)n(l)dl$. Within the volume between the coil ends the product $B(l)n(l)$ is essentially constant, and rapidly decreases beyond the ends. Therefore, the rotation occurs almost entirely between the ends, with negligible contribution beyond the ends. The midpoint B and n are referred to here and prevail over 75% of the length l ; over the remainder of the length increasing B is compensated by decreasing n . Separate determination of n makes possible calculation of B from the observed θ_r . Here n is inferred from a separate 3.39μ infrared interferometer measurement⁶ of initial electron density of $6 \times 10^{15}/\text{cm}^3$, and the Kerr cell observation of compression to $\frac{1}{4}$ of the initial radius, yielding 1×10^{17} . Therefore, a forward magnetic field of 20 000 gauss is deduced to prevail on the central axis within the column. This field is much less than the 50 000-gauss compression field which is present outside the column, and also much less than the calculated value of a completely trapped and compressed bias field. With the maser beam positioned parallel to and 1 cm from the coil axis, which is $\frac{1}{2}$ cm beyond the periphery of the plasma column, where the compression field is 50 kG, no rotation was observed. This indicates that the electron density along the beam is less than $1/30$ of that within the column.

This method used in conjunction with interferometric techniques⁶⁻⁸ for separate measurement of electron density realizes quantitative measurement with time and space resolution of magnetic fields in dense, hot, dynamical plasmas.

*Research supported by the U. S. Air Force Aerospace Research Laboratories and the National Science

Foundation.

¹Arwin A. Dougal, Bull. Am. Phys. Soc. 8, 163 (1963).

²Arwin A. Dougal, Proceedings of the Fourth Symposium on MHD, IEEE, New York, New York, 1963 (unpublished).

³John P. Craig, Robert F. Gribble, and Arwin A. Dougal, to be published.

⁴Robert F. Gribble and Arwin A. Dougal, Bull. Am.

Phys. Soc. 9, 315 (1964).

⁵R. F. Gribble and Arwin A. Dougal, Bull. Am. Phys. Soc. 8, 131 (1963).

⁶R. F. Gribble, J. P. Craig, and Arwin A. Dougal, to be published.

⁷F. C. Jahoda, W. E. Quinn, and F. L. Ribe, Bull. Am. Phys. Soc. 9, 311 (1964).

⁸G. A. Sawyer, W. E. Quinn, and F. L. Ribe, Bull. Am. Phys. Soc. 9, 311 (1964).

ANTIFERROMAGNETIC ORDERING IN AN ISING LATTICE BY A MONTE CARLO METHOD

E. A. Harris

Clarendon Laboratory, Oxford, England

(Received 1 June 1964)

The magnetic properties of face-centered cubic antiferromagnetic crystals do not agree well with simple molecular field theory, and a spin-wave approach is only reliable at very low temperatures. For this reason an attempt to understand the apparently anomalous magnetic properties¹ of MnO in the region of the transition temperature has been made by an extension of the molecular field approach using a Monte Carlo method. This method of treating problems in statistical mechanics, which is made feasible only by the use of a high-speed computer, was first used by Metropolis and others² and has been applied to ordering in crystal lattices by Ehrman, Fosdick, and Handscomb³ and by Handscomb.⁴

In the simplest molecular field approximation, the exchange interactions between a spin and its neighbors are replaced by an effective field which is proportional to the sublattice magnetization. MnO has type-II order so that any spin has its 6 next nearest neighbors (n.n.n.) all antiparallel, but of its 12 nearest neighbors (n.n.) 6 are parallel and 6 antiparallel. This means that the n.n. do not contribute to the effective field, which is given by

$$g\beta H_E = 6J_2 \langle S_z \rangle,$$

where the n.n.n. interaction is of the form $J_2 \vec{s}_i \cdot \vec{s}_j$. So in this approximation, the magnetic properties should be independent of the n.n. interaction. In reality, as the temperature rises from zero, n.n. interactions must lead to short-range n.n. ordering, and this increases with temperature, eventually destroying the long-range order at a lower temperature than that predicted by the simple theory. The present method allows for this.

The calculation proceeds as follows:

(1) Each spin in a block of 384 spins forming a

fcc lattice is represented by a variable in the computer. Continuity at the boundaries of the block is obtained by linking the top to the bottom, the left-hand side to the right-hand side, and so on. Each of these variables can take one of the $2S+1$ values, $M_i = -S, -S+1, \dots, +S$, and the configuration at any moment is specified by these 384 numbers.

(2) Some initial configuration is set up, either ordered or disordered.

(3) Each site is now considered in turn. (a) The effective field at site i is computed in terms of the magnetic quantum numbers of its 12 n.n. (M_j) and 6 n.n.n. (M_k):

$$g\beta H_E = J_1 \sum_j M_j + J_2 \sum_k M_k.$$

(b) The energies of the possible states for M_i are computed:

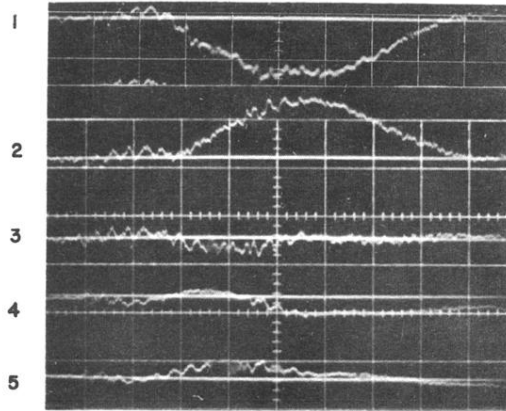
$$E_i = g\beta H_E M_i.$$

(c) A new value for M_i is selected by a pseudo-random process such that the probability of selecting any particular value is proportional to

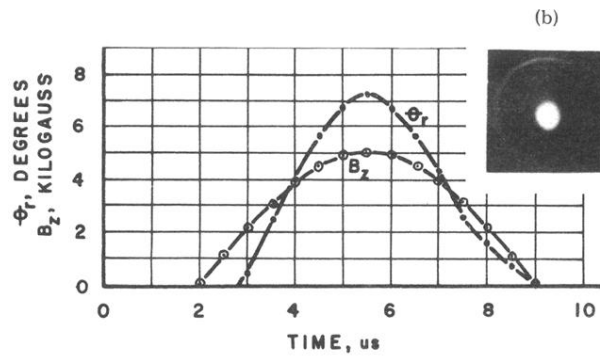
$$P = e^{-E_i/kT}.$$

It is this new value which is used when treating subsequent sites. When all 384 sites have been considered, the whole cycle is repeated.

(4) At the end of each cycle, information is extracted about the state of magnetic ordering. In order to allow for different types of order, the lattice is divided into 32 sublattices, so that no spin lies on the same sublattice as any of its n.n. or n.n.n. The magnetization $\langle M_i \rangle$ is computed for each sublattice. A long-range ordering parameter is defined as the average of the moduli of these. Short-range ordering is measured



(a)



(c)

FIG. 2. Faraday-rotation results for beam positioned on central axis. Traces 2 and 4 of (a), $1 \mu\text{sec}/\text{div}$, are difference and sum, respectively. Trace 1 is a repeat difference for the analyzer rotated 90° . Traces 3 and 5 are difference and sum in the absence of the maser beam. Amplitudes are $250 \mu\text{V}/\text{div}$ and $1.25 \text{ mV}/\text{div}$ for the difference and sum traces, respectively. (b) is a Kerr cell photograph of the compressed plasma column at the instant of peak compressing field. θ_r of (c) is calculated from traces 2 and 5 and plotted with the compression field of 50-kG peak.